# Extended Energy Spectrum Measurements Of Elements With The Cosmic Ray Isotope Spectrometer (CRIS)

A.W. Labrador[1], N.E. Yanasak[2], W.R. Binns[3], A.C. Cummings[1], G.A. de Nolfo[4], J.S. George[1], M.H. Israel[3], R.A. Leske[1], M. Lijowski[3], R.A. Mewaldt[1], E.C. Stone[1], T.T. von Rosenvinge[4], M.E. Wiedenbeck[2]
*(1) California Institute of Technology, Pasadena, CA 91125 USA*
*(2) Jet Propulsion Laboratory, Pasadena, CA 91109 USA*
*(3) Washington University, St. Louis, MO 63130 USA*
*(4) NASA/Goddard Space Flight Center, Greenbelt, MD 20771 USA*

## Abstract

We describe a multiple dE/dx technique used to identify particles that penetrate through the bottom of the CRIS instrument, significantly extending the measured energy ranges for major elements beyond that for stopping particles. In preliminary analysis, the upper energy limit for oxygen has been extended from ∼240 MeV/nuc for stopping particles to ∼ 410 MeV/nuc for penetrating particles, and the upper energy limit for iron has been extended from ∼470 MeV/nuc to ∼ 670 MeV/nuc. We report new element intensities in these extended energy ranges, and compare them with previously reported intensities and with spectra derived using cosmic ray transport and solar modulation models.

## 1. Introduction

The Cosmic Ray Isotope Spectrometer (CRIS) aboard the Advanced Composition Explorer (ACE) has been measuring galactic cosmic ray abundances since ACE was launched in August 1997. CRIS is a silicon detector telescope which identifies charged particles via the ΔE vs. E′ ("residual E") technique, and to date, energy spectra reported by CRIS have been limited to those particles that stop in the instrument. Although stopping particles are required for isotopic resolution, elemental spectra can be obtained at higher energies using penetrating particles.

The CRIS instrument is composed of four identical silicon detector stacks, topped by a scintillating optical fiber trajectory (SOFT) system. Each detector stack is composed of 9 circular silicon detectors, labeled E1 through E9. The instrument is described in detail in [3].

Particles that enter the instrument through E1 are assigned a range flag (RNG) corresponding to the deepest detector in the stack that detects a hit, so a particle that stops in E8 is assigned RNG 8. Any particle with RNG≤ 8 is

pp. 1773–1776 

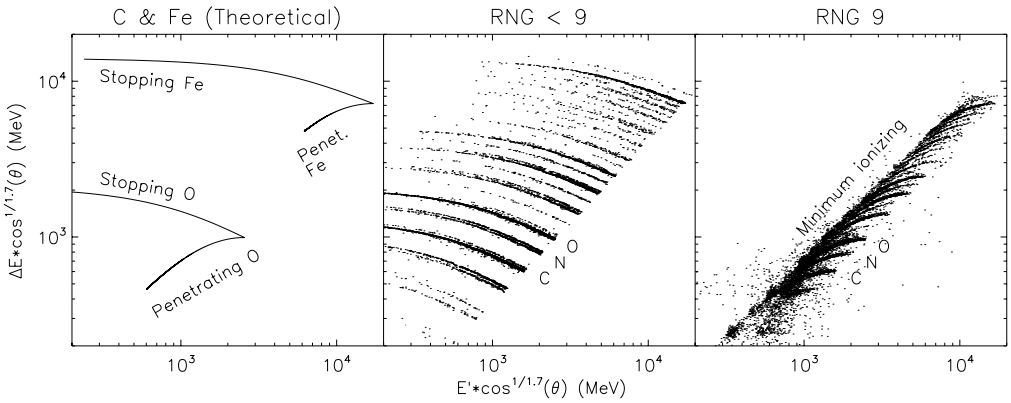


**Fig. 1.** ΔE vs. E′ sample data measured by CRIS. The left panel shows calculated responses for O and Fe, for stopping and penetrating particles. The center and right panels show sample flight data for stopping and penetrating particles, respectively. C, N, and O are identified. The $\cos^{1/1.7}(\theta)$ factors adjust for angle of incidence and assume the range-energy relationship is approximated by a power law.

treated as a stopping particle. Particles that stop in E9 or penetrate through the bottom of E9 are designated as penetrating particles, or RNG 9. The left panel of Figure 1 shows the expected responses for stopping and penetrating oxygen and iron in the CRIS instrument, via the ΔE vs. E′ technique. In Figure 1, ΔE is the measured energy deposited in E1 through E4, and E′ is the measured energy deposited in E5 through E8. Other combinations of ΔE and E′ are possible; this combination is selected for illustration. The fold-back point of each curve is the point at which the particles leave E8 and enter E9. The left-most points along the penetrating particle curves are the minimum ionizing points. The center panel of Figure 1 shows particle identification for a sample of flight data. Charge and isotope separation are clearly evident, and it is particles in these ranges that have been analyzed to date, e.g. [4].

## 2. Analysis

RNG 9 particles are shown in the right panel of Figure 1, and charge separation is still clearly evident up until the energies approach the minimum ionizing energies shown as the diagonal band in the figure. In the penetrating particle analysis, particles are selected from the ΔE vs. E′ regions where charge separation is clearly evident, e.g. well to the right of the minimum ionizing band. For the present analysis, we concentrate on the relatively abundant elements (e.g. C, N, O) which would be less affected by background or by contamination from adjacent charges.

Energy ranges must be determined for each charge, Z, in order to calculate fluxes. We employ a range-energy relationship for hydrogen passing through silicon and scale for higher Z [1,2,3]. From these range-energy relationships, we

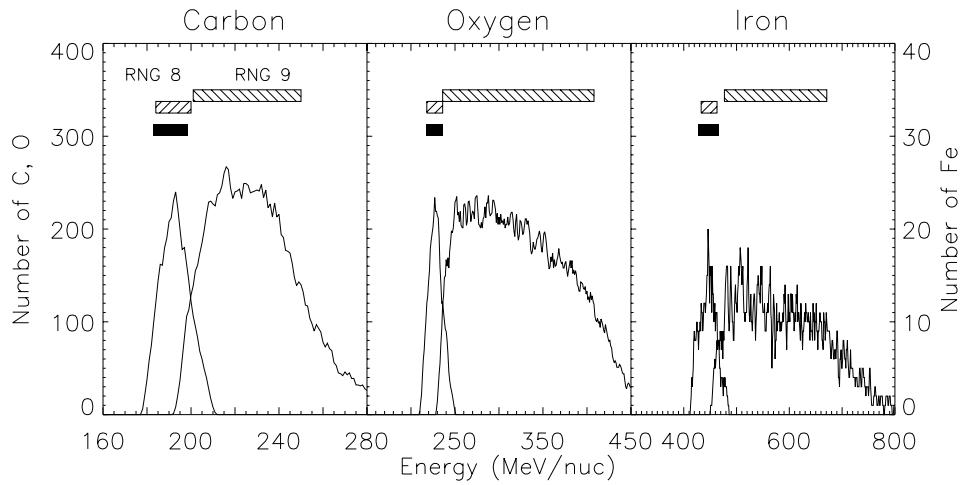


**Fig. 2.** Energy histograms for C, O, and Fe for sample flight data. RNG 8 and RNG 9 energy histograms are shown in each panel, using penetrating particle analysis. The horizontal black bars show RNG 8 energy range from stopping analysis, while the shaded bars show RNG 8 and 9 energy ranges using the penetrating particle analysis.

calculate expected CRIS detector responses for various values of Z, mass A, and incident energy. Because particles are selected from the $\Delta$E vs. E$'$ regions where charges are well separated, charges are assigned to particles based on their $\Delta$E and E$'$ values, and we assume the most abundant cosmic ray mass values for each element. Finally, for each particle, we find the best-fit incident energy corresponding to the given Z, A, and detector responses, taking into account measured angle of incidence and dead layer thicknesses.

Figure 2 shows the resulting smoothed energy histograms for C, O, and Fe, for a flight data sample. To check the algorithm, we have also applied the penetrating particle analysis to RNG 8 particles, treating E7 as the bottom detector and ignoring E8. Energy ranges are taken to be the FWHM of the histograms. The RNG 8 "penetrating" energy ranges compare well with RNG 8 stopping energy ranges for abundant elements like C and O and less well with Fe, which could benefit from further analysis. However, this initial comparison implies that the RNG 9 energy range from penetrating particle analysis is reasonable.

## 3. Results

Figure 3 compares our penetrating particle energy ranges with the energy ranges from stopping particle analysis, for C, N, O, Ne, Si, and Fe. This initial penetrating particle analysis extends the currently available energy ranges (RNG $2-8$) by $\sim 30\%$ to $\sim 120\%$, depending on charge.

Figure 4 shows penetrating particle fluxes for Bartels rotations $2241-2242$, along with publicly available CRIS data (http://www.srl.caltech.edu/ACE/ASC/)

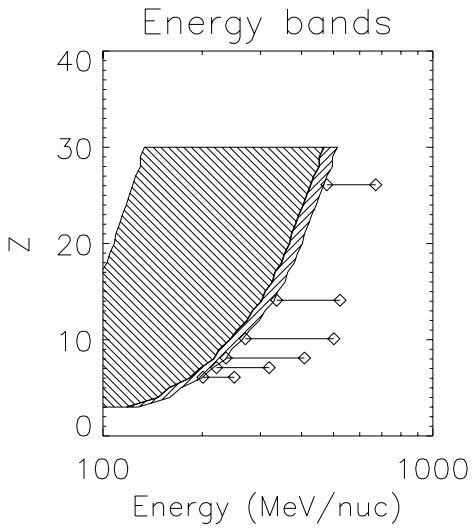


**Fig. 3.** Energy bands for the CRIS instrument for $Z = 3 - 30$. The left shaded region is for RNG $2 - 7$ stopping particles, and the right shaded region is for RNG 8. The horizontal lines show energy ranges for penetrating (RNG 9) C, N, O, Ne, Si, and Fe.

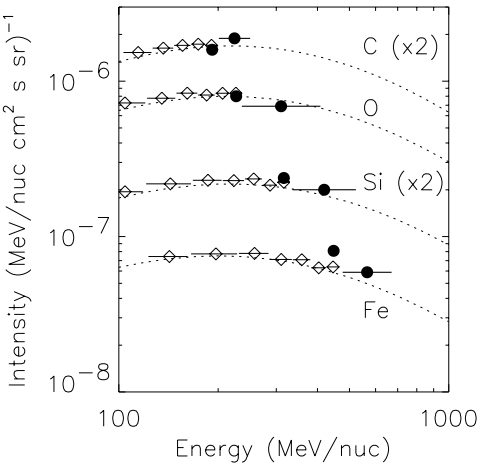


**Fig. 4.** Element spectra for C, O, Si, and Fe measured by CRIS for Bartels rotations $2241 - 2242$. The open diamonds are publicly available data (stopping particles). The filled circles are RNG 8 and penetrating particle fluxes using energy ranges determined by the penetrating particle analysis. Uncertainties are smaller than plot symbols.

from the same period and calculated galactic cosmic ray spectra. When compared with the available data, the penetrating particle fluxes appear most reasonable for O and Si. For carbon, there is still some contamination from minimum ionizing particles which must be eliminated with further refinements of the selection criteria (see Figure 1). For iron, the deviation of the RNG 8 "penetrating" flux from the RNG 8 stopping flux is due primarily to the wider "penetrating" energy range, which could be refined in further analysis.

*Acknowledgments*: This work was supported by NASA at Caltech (under grant NAG5-6912), JPL, Washington University, and GSFC.

## 4. References

1. Ahlen, S.P. 1980, Rev. Mod. Phys, 52, 121.
2. Andersen, H.H. and Ziegler, Z.F. 1977, "Hydrogen: Stopping Powers and Ranges in All Elements", Volume 3 of The Stopping and Ranges of Ions in Matter, (Pergamon: New York)
3. Stone, E.C. et al. 1998, Space Sci. Rev., 96, 285.
4. Wiedenbeck, M.E. et al. 2000, AIP Conf. Proc., 516, 301.